Available online at www.sciencedirect.com
ScienceDirect
Biomaterials 29 (2008) 2203–2216
Biomaterials
www.elsevier.com/locate/biomaterials

The influence of proepicardial cells on the osteogenic potential of marrow stromal cells in a three-dimensional tubular scaffold

Mani T. Valarmathi [a,*], Michael J. Yost [b], Richard L. Goodwin [a], Jay D. Potts [a]

[a] Department of Cell and Developmental Biology & Anatomy, School of Medicine, University of South Carolina, Columbia, South Carolina, USA
[b] Department of Surgery, School of Medicine, University of South Carolina, Columbia, South Carolina, USA

Received 12 November 2007; accepted 27 January 2008
Available online 19 February 2008

Abstract

It is well established that the process of neovascularization or neoangiogenesis is coupled to the development and maturation of bone. Bone marrow stromal cells (BMSCs) or mesenchymal stem cells (MSCs) comprise a heterogeneous population of cells that can be differentiated in vitro into both mesenchymal and non-mesenchymal cell lineages. When both rat BMSCs and quail proepicardia (PEs) were seeded onto a three-dimensional (3-D) tubular scaffold engineered from aligned collagen type I strands and co-cultured in osteogenic media, the maturation and co-differentiation into osteoblastic and vascular cell lineages were observed. In addition, these cells produced abundant mineralized extracellular matrix materials and vessel-like structures. BMSCs were seeded at a density of 2×10^6 cells/15 mm tube and cultured in basal media for 3 days. Subsequently, on day 3, PEs were seeded onto the same tubes and the co-culture was continued for another 3, 6 or 9 days either in basal or in osteogenic media. Differentiated cells were subjected to immunohistochemical, cytochemical and biochemical analyses. Phenotypic induction was analyzed at mRNA level by reverse transcriptase quantitative polymerase chain reaction (RT-qPCR). Immunolocalization of key osteogenic and vasculogenic lineage specific markers were examined using confocal scanning laser microscopy. In osteogenic tube cultures, both early and late osteogenic markers were observed and were reminiscent of in vivo expression pattern. Alkaline phosphatase activity and calcium content significantly increased over the observed period of time in osteogenic medium. Abundant interlacing fascicles of QCPN, QH1, isolectin and α-smooth muscle actin (α-SMA) positive cells were observed in these tube cultures. These cells formed extensive arborizations of nascent capillary-like structures and were seen amidst the developing osteoblasts in osteogenic cultures. The 3-D culture system not only generated de novo vessel-like structures but also augmented the maturation and differentiation of BMSCs into osteoblasts. Thus, this novel co-culture system provides a useful in vitro model to investigate the functional role and effects of neovascularization in the proliferation, differentiation and maturation of BMSC derived osteoblasts.

Keywords: Bone marrow stromal cells; Mesenchymal stem cells; Proepicardial cells; Osteogenesis; Vasculogenesis; Bone tissue engineering

1. Introduction

The first evidence that postnatal bone marrow stroma contains precursor cells for non-hematopoietic mesenchymal tissues came from the work of Friedenstein and co-workers [1,2]. The precursor cells were initially referred to as colony-forming units-fibroblast (CFU-F) and, later as marrow stromal cells or mesenchymal stem cells. Stromal stem cells are multipotent, present throughout the lifespan of an organism, and give rise to the support cells of the bone marrow, including colonies of osteoblasts, chondroblasts and adipocytes [3–5].

Directed differentiation of BMSCs into the osteogenic lineage in vitro can be facilitated by culturing these cells in the presence of dexamethasone, β-glycerol phosphate and ascorbic acid [6]. Bone morphogenetic and osteogenic proteins (BMPs/OPs), members of the transforming growth factor β (TGF-β)

* Corresponding author. Building 1 Room B-60, 6439 Garners Ferry Road, Department of Cell and Developmental Biology & Anatomy, School of Medicine, University of South Carolina, Columbia, South Carolina 29209, USA. Tel.: +1 803 733 3294; fax: +1 803 733 3212.
E-mail addresses: valarmathi64@hotmail.com, valarmathi@gw.med.sc.edu (M.T. Valarmathi).

0142-9612/$ - see front matter © 2008 Elsevier Ltd. All rights reserved.
doi:10.1016/j.biomaterials.2008.01.025

super family, are soluble mediators of tissue morphogenesis and induce de novo endochondral bone formation in heterotopic extraskeletal sites [7]. Soluble molecular signals induce morphogenesis and work in conjunction with the geometric topography of the extracellular substratum dictates the biological pattern formation and bone development [8].

Angiogenesis and vascular invasion are a prerequisite to the process of osteogenesis, both in development and during repair [9,10]. Developing vascularized tissue in vitro is important for clinical and surgical implications and is also essential for the viability and functional integrity of any engineered tissue or organ [11]. Vascular cells have dramatic inductive osteogenic effects [12]; reciprocally osteogenesis induces the expression of angiogenic factors [13].

Perez-Pomares et al. have proposed proepicardium (PE) as a suitable cellular source for vascular tissue engineering [14]. The PE contains all the cellular precursors for coronary vessel development [15–17] and displays a high vasculogenic potential, both in vivo (as shown by heterotopic transplants) and in vitro [18,19].

The purpose of this study was to determine the effect of neovascularization on the osteogenic differentiation potential of BMSCs when co-cultured with PEs in osteoinductive media. Cultures were grown on a three-dimensional (3-D) collagen scaffold that supports coronary vessel development. In this osteogenic culture condition, cells matured and co-differentiated into osteoblastic or vascular cell lineages. In addition, these cells produced abundant mineralized extracellular matrix materials and showed vascular morphogenesis. Our experiments indicate that co-culture of PEs and BMSCs augmented the expression of bone-related proteins.

It is well established that extracellular matrix (ECM) components play a critical role in morphogenesis. ECM molecules have potent effects on cell proliferation and differentiation, and direct the assembly of 3-D tissues in vitro. Our results indicate that the specific geometrical alignment of collagen strands in our 3-D tubular scaffold [20] provides a conducive microenvironment that allows for the differentiation of vascularized bone-like tissue. Thus, this unique co-culture system provides an in vitro model to investigate the functional role and effects of neovascularization in the maturation and differentiation of BMSC derived osteoblasts as well as the formation of mature bone.

2. Materials and methods

2.1. Production of tubular scaffold

The 3-D collagen type I tube served as a scaffold on which rat BMSC and quail PE co-cultures were carried out. The details of the production and properties of the collagen tubes have previously been described [20]. Briefly, a 25 mg/ml solution of bovine collagen type I was extruded with a device that contained two counter-rotating cones. The liquid collagen was fed between the two cones and forced through a circular annulus in the presence of a NH_3–air (50–50 vol/vol) chamber. This process results in a tube of aligned collagen fibrils. The dimensions of tubes produced for this set of experiments had a length of 15 mm with a luminal diameter of 4 mm and an exterior diameter of 5 mm, leaving a wall thickness of 1 mm. The collagen tubes had a defined fiber angle of 18° relative to the central axis of the tube and had pores ranging from 1 to 10 μm. The tubes were sterilized using Stratalinker UV crosslinker 1800 (Stratagene) and then placed in Mosconas solution (in mM: 136.8 NaCl, 28.6 KCl, 11.9 $NaHCO_3$, 9.4 glucose, 0.08 NaH_2PO_4, pH 7.4) (Sigma–Aldrich) containing 1 μl/ml gentamicin (Sigma–Aldrich) and incubated in 5% CO_2 at 37 °C until cellular seeding.

2.2. BMSC isolation, expansion and maintenance (nonclonal BMSC culture)

The procedures were performed in accordance with the guidelines for animal experimentation by the Institutional Animal Care and Use Committee, School of Medicine, University of South Carolina. Rat BMSCs were isolated from the bone marrow of young adult 80 g male Wister rats (Harlan Sprague Dawley, Inc.). Briefly, after deep euthanasia and cervical dislocation, the femoral and tibial bones were removed aseptically and cleaned extensively to remove associated soft connective tissues. The marrow cavities of these bones were flushed with Dulbecco's Modified Eagle Medium (DMEM; Invitrogen) and combined. The obtained marrow plugs were triturated and passed through needles of decreasing gauge (18 down through 22 gauge) to break up clumps and cellular aggregates. The resulting single-cell suspensions were centrifuged at 200 g for 5 min. Nucleated cells were counted using a hemocytometer. Cells were plated at a density of 5×10^6–2×10^7 cells per T75 cm^2 flasks in basal media composed of DMEM supplemented with 10% FBS (lot-selected; Hyclone), gentamicin (50 μg/ml) and amphotericin B (250 ng/ml) and incubated in a humidified atmosphere of 5% CO_2 at 37 °C for 7 days. The medium was replaced, and changed three times per week until the cultures become ~70% confluent (between 12 and 14 days). Cells were trypsinized using 0.05% trypsin–0.1% EDTA and re-plated at a density of 1×10^6 cells per T75 cm^2 flasks. After three passages, attached marrow stromal cells were devoid of any non-adhering population of cells.

2.3. Clonal BMSC culture

Single-cell suspensions of BMSCs prepared as described above were plated in 150 mm × 20 mm Petri dishes at a low density of 1–4×10^3 nucleated cells/cm^2. After 24 h of incubation, the cultures were thoroughly washed with complete DMEM to remove nonadherent cells. The cultures were continued as described above for 12–14 days. Colonies that were well defined and separated from neighboring colonies were washed with Mosconas solution (pH 7.4) and individual colonies were isolated using a cloning cylinders (Sigma–Aldrich). Cells were trypsinized and re-plated onto individual wells of a six-well culture plates. At approximately 80% confluency, the subcultured cells were transferred to T25 cm^2 followed by T75 cm^2 (passage 3) flasks and expanded to confluency.

2.4. Phenotypic characterization of BMSCs by flow cytometry

Quantitative analysis of various cell surface markers was performed by flow cytometry using a Coulter® EPICS® XL™ Flow Cytometer. Briefly, the passage 3 maintained BMSCs were trypsinized, pelleted at 200 g for 5 min and washed twice with phosphate buffered saline (PBS), pH 7.4. Cells were re-suspended in staining buffer (PBS, 0.1% NaN_3, 1% FBS) and incubated for 30 min at 4 °C with appropriate dilutions of FITC-conjugated mouse anti-rat CD11b, CD45, CD90 or OX43 monoclonal antibodies (Table 1). Mouse anti-rat FITC-IgG antibody served as the isotype control. Cells were washed twice with staining buffer and either acquired immediately or fixed in ice-cold 0.5% paraformaldehyde (Sigma–Aldrich) and stored in the dark at 4 °C until acquired in flow cytometry. The acquired data were analyzed using SYSTEM II software (Beckman Coulter).

2.5. Quail PE isolation

Pharaoh Quail eggs (Lake Cumberland, NC) were incubated at 38 °C for 65 h. Quail embryos staged according to Hamburger–Hamilton Staging (HH16–HH17) [21] were isolated and placed in Tyrode's buffer. The membranes around the embryo and heart were reflected back and the proepicardium was dissected using fine forceps.

Table 1
Primary antibodies used in this study

Primary antibodies	Dilutions	Source	Cell target
Characterization markers			
CD11b	1:250	BD Pharmingen	Leukocytes
CD45	1:250	BD Pharmingen	Hematopoietic
CD90	1:250	BD Pharmingen	BMSCs
OX43	1:50	Gene Tex, Inc	Endothelial
Osteogenic markers			
Osteonectin	1:100	DSHB	Osteoblasts
Osteopontin	1:100	DSHB	Osteoblasts
Osteocalcin	1:100	Santa Cruz Biotechnology	Osteoblasts
Alkaline phosphatase	1:100	R&D System	Osteoblasts
Vasculogenic markers			
QCPN	1:100	DSHB	Quail Cells
QH1	1:100	DSHB	Quail endothelial
Isolectin	1:100	Invitrogen	Endothelial
α-SMA	1:100	Sigma–Aldrich	Smooth muscle

2.6. BMSCs and PEs co-culture

Clonally expanded passage 3 BMSCs were seeded into the tubular scaffolds at a density of 2×10^6 cells/15 mm tube by pipetting directly into the tubes and cultured in basal media. On day 3 the majority of the media was removed from the BMSC tube culture and two proepicardial organs were allowed to adhere to the tube surface for 12–16 h. After 12–16 h, fresh media was again added to the cultures.

2.7. Osteogenic differentiation

All explants and tubes were cultured either in basal media or in osteogenic media consisting of DMEM supplemented with 10% FBS, 10 mM sodium β-glycerol phosphate (Sigma–Aldrich), 50 μg/ml L-ascorbic acid (Sigma–Aldrich), 10^{-8} M dexamethasone (Sigma–Aldrich) and 8 μg/ml gentamicin for 3, 6 or 9 days. In addition, BMSCs (clonally expanded passage 3) only were seeded in tubular scaffolds at a density of 2×10^6 cells/15 mm tube and cultured either in basal media or in osteogenic media for 3, 6 or 9 days. The cultures were terminated at these intervals and subsequently processed for RT-qPCR, immunohistochemical, cytochemical and biochemical analyses.

2.8. Real-time quantitative RT-PCR (RT-qPCR) analysis

Total cellular RNA extraction from three independent collagen tube cultures/co-cultures maintained both in basal and in osteogenic media were performed using TRIzol® Plus RNA purification kit (Invitrogen) according to manufacturer's instructions. The quality and quantity of the obtained RNA were analyzed on the Agilent 2100 Bioanalyzer using the Agilent RNA 6000 nanokit (Agilent Technologies, Inc.) according to manufacturer's instructions. The reverse transcriptase (RT) reaction was performed using 500 ng of total RNA in a final volume of 20 μl using an iScript™ cDNA synthesis kit (Bio-rad Laboratories) according to manufacturer's recommendations.

Highly purified desalted gene-specific primers for collagen 1α (Col1a1), osteonectin (Sparc), osteopontin (Spp1), osteocalcin (Bglap2), runx2 (Runx2) and the calibrator reference gene, acidic ribosomal phosphoprotein P0 (Arbp), were designed using web based software (http://frodo.wi.mit.edu/cgi-bin/primer3/primer3_www.cgi), synthesized commercially (Integrated DNA Technologies, Inc.), and evaluated for an annealing temperature of 58 °C as shown in Table 2.

Real-time PCR conditions were optimized as described previously [22]. All RT-qPCRs were performed with SYBR Green I chemistry in an iQ5 real-time PCR detection system (Bio-Rad Laboratories). For qPCRs, iQ5 SYBR Green I supermix, 3 pmol/μl of each forward and reverse primers and 5 μl cDNA template were used in a final reaction volume of 50 μl and plates were loaded using a RT loading platform. Cycling conditions included an initial denaturation step of 8 min and 45 s at 95 °C followed by 45 cycles of 30 s at 95 °C, 30 s at 58 °C, and 30 s at 72 °C. Data collection was enabled at 72 °C in each cycle. C_T (threshold cycle) values were calculated using the iQ5 optical system software version 2.

Quantification of gene expression was based on the C_T value for each sample using Relative Expression Software Tool (REST©). C_T values were calculated as the average of three replicate measurements for each sample analyzed. The mathematical model previously described in detail [23–25] (http://www.wzw.tum.de/gene-quantification/) was used to determine the expression ratio of genes.

The mathematical equation used to calculate an expression ratio includes an efficiency correction for real-time PCR efficiency of the individual transcripts.

$$R = \frac{\left(E_{\text{target}}\right)^{\Delta \text{CP}_{\text{target}}\left(\text{MEAN}_{\text{control}} - \text{MEAN}_{\text{sample}}\right)}}{\left(E_{\text{ref}}\right)^{\Delta \text{CP}_{\text{ref}}\left(\text{MEAN}_{\text{control}} - \text{MEAN}_{\text{sample}}\right)}}$$

The relative expression ratio of a target gene was computed, based on its real-time PCR efficiencies (E) and the crossing point (CP) difference (Δ) of an unknown sample versus a control ($\Delta \text{CP}_{\text{control}-\text{sample}}$). The calibrator control included passage 3 BMSCs day 0 sample. In mathematical models the target gene expression was normalized by a non-regulated reference gene expression, Arbp. Finally, the differences in expression of the investigated transcripts between control and treated samples were assessed in group means for statistical significance by applying *'Pair Wise Fixed Reallocation Randomization Test'* for each sample and a value of $p < 0.05$ was regarded as significant.

2.9. Immunostaining and confocal microscopy

Collagen tube constructs containing BMSCs and PEs were collected and fixed in 2% paraformaldehyde at 4 °C for 12–16 h [26]. Each of the samples was then permeabilized in PBS, pH 7.4, containing 0.1% Triton X-100 (Sigma–Aldrich) and 100 mM glycine (Sigma–Aldrich) for 30 min and blocked in 1.5% bovine serum albumin (BSA, Sigma–Alrich), 0.5 mM glycine in PBS for 1 h at room temperature. The primary antibodies used are summarized in Table 1. Secondary antibodies (Alexa 488, 546, 633 obtained from Molecular Probes, Invitrogen) were used at 1:100 dilutions in blocking buffer for 1–2 h at room temperature. The *Griffonia simplicifolia* isolectin GS-IB_4 (1:100 in 1.5% BSA/PBS; Invitrogen) was used to identify endothelial cell.

Table 2
RT-qPCR primer sequences used in this study

Genes	Forward primer	Reverse primer	Product length (bp)	Annealing temperature (°C)	Genbank accession no
Col1a1	5′-TCCTGCCGATGTCGCTATC-3′	5′-CAAGTTCCGGTGTGACTCGTG-3′	234	58	XM_213440
Sparc	5′-ACAAGCTCCACCTGGACTACA-3′	5′-TCTTCTTCACACGCAGTTT-3′	180	58	NM_012656
Spp1	5′-GACGGCCGAGGTGATAGCTT-3′	5′-CATGGCTGGTCTTCCCGTTGC-3′	208	58	NM_012881
Bglap2	5′-AAAGCCCAGCGACTCT-3′	5′-CTAAACGGTGGTGCCATAGAT-3′	232	58	NM_013414
Runx2	5′-GCTTCTCCAACCCACGAATG-3′	5′-GAACTGATAGGACGCTGACGA-3′	212	58	XM_346016
Arbp	5′-CGACCTGGAAGTCCAACTAC-3′	5′-ATCTGCTGCATCTGCTTG-3′	109	58	Z29530

Alexa 488 phalloidin (1:200 in PBS) was used to stain filamentous actin. Nuclei were stained with DAPI (4′,6-diamidino-2-phenylindole, 100 ng/ml). Images of the collagen tubular constructs were obtained using a Zeiss LSM 510 Meta confocal scanning laser microscope. Negative control for staining included only secondary antibodies.

2.10. Alizarin red S staining for calcium

Collagen tube cultures under osteogenic differentiation conditions with and without the seeding of BMSCs were processed for confocal microscopy as above and stained with 0.1% Alizarin red S, pH 4.1–4.3 (Sigma–Aldrich). This is performed to visualize areas of mineralization and nodule formation.

2.11. Alkaline phosphatase assay

The DNA content and alkaline phosphatase activity were measured as described previously [27]. Production of alkaline phosphatase was measured using a plate reader (Bio-rad, Bench Mark Plus, Microplate Spectrophotometer). Tube cultures at various time points (3, 6, 9, 12, 15 or 18 days) maintained as replicates were washed twice with PBS, pH 7.4, and frozen at −70 °C. Upon thawing, the tubes were homogenized with 0.5 ml of Tris buffer (pH 8.8; Sigma–Aldrich). The samples were sonicated for 5 min on ice, after which an aliquot of sonicated cell suspension was used for DNA quantification. Quantification of the DNA content was determined using Quant-iT PicoGreen dsDNA Reagent Kits (Molecular Probes) according to manufacturer's instructions. To measure alkaline phosphatase activity, the same sonicated cell suspension was centrifuged at 13,000g for 1 min at 4 °C. Aliquots of 5 μl supernatant were analyzed using QuantiChrom™ Alkaline Phosphatase Assay Kit (DALP-250) according to manufacturer's instructions (BioAssay Systems). The absorbance was recorded at 405 nm at time zero ($t = 0$), and again after 4 min ($t = 4$) on a plate reader. The samples were maintained at 37 °C between readings. Enzyme activity was expressed as *p*-nitrophenol μmol/min/10^7 cells.

2.12. Calcium assay

The tube cultures at various time points (3, 6, 9, 12, 15 or 18 days) maintained as replicates were rinsed twice with PBS, pH 7.4, and homogenized with 0.5 ml of Tris buffer (pH 8.8). Then, the samples were sonicated for 5 min on ice and centrifuged at 1000g for 5 min. The resulting supernatant (5 μl) was used for calcium determination using QuantiChrom™ Calcium Assay Kit (DICA-500) according to manufacturer's instructions (BioAssay Systems). Absorbance of samples was read at 612 nm, 3 min after the addition of reagents. Total calcium was determined using the standard solutions prepared in parallel, and expressed in mg/dL/tube.

2.13. Statistical analysis

Results were represented by mean ± standard error of the mean (SEM). The results of the biochemical assays were grouped by day for the various culture conditions and the data were analyzed by ANOVA using SigmaStat 3.5 software. Values of $p < 0.05$ were considered statistically significant.

3. Results

3.1. Phenotypic characterization of input BMSCs

Analysis of cell surface markers by flow cytometry on passage 3 BMSCs revealed that the intensity and distribution of the cells stained for CD11b (integrin α_m chain, Mac-1 α chain; Fig. 1B), CD45 (leukocyte common antigen; Fig. 1C) and OX43 (antigen expressed in all vascular endothelial cells of rat; Fig. 1D) were not significantly different from those of isotype control (Fig. 1A), signifying that the these cultures were devoid of any potential hematopoietic stem and/or progenitor cells as well as endothelial cells. In contrast, BMSCs were found to express the surface antigen CD90 (Thy-1; Fig. 1E), consistent with their undifferentiated state. Phenotypic characterization and evaluation of these markers on clonally expanded BMSCs showed expression patterns consistent with their parent culture. Expression patterns of these surface molecules were consistent with previous reports [28].

3.2. RT-qPCR analysis of osteogenic markers

In order to compare the differential gene expression profile between BMSCs/PEs co-culture and BMSC culture, real-time quantitative RT-PCR (RT-qPCR) analyses of osteoblastic differentiation markers were carried out at the defined time points (3, 6 or 9 days) on BMSCs/PEs co-cultured in tubular scaffold either in basal or in osteogenic media. Additionally, RT-qPCR on BMSCs cultured in the tubular scaffolds in the same media conditions was performed at the same time points. Identical time points were chosen for BMSCs/PEs co-cultures and BMSC cultures and, this was based on the stage of mineralization observed in osteogenic culture conditions. Mineralization was evident around day 9 in these tube cultures.

The expression pattern of key osteogenic gene transcripts in tube cultures showed a dramatic difference in response to basal and osteogenic media (Fig. 2A–D). In BMSC/PE co-culture in basal media, collagen type I remained at basal level. Osteonectin and Runx2 were upregulated at day 3 and day 9, both transcripts showed a transient downregulation during day 6. Osteopontin and osteocalcin remained upregulated beyond day 3 (Fig. 2A). When BMSCs/PEs were co-cultured on the tubular scaffold in osteogenic media, the transcripts level of collagen type I showed an initial upregulation which returned to the baseline level after 6 days. Osteonectin and Runx2 showed slight upregulation over day 9. Osteopontin, the early osteogenic marker, showed sustained marked upregulation over 9 days and osteocalcin, the late stage osteogenic marker, showed a gradual upregulation with a marked increase at day 6 which was augmented through day 9 (Fig. 2B).

In comparison, osteogenic tube cultures of BMSCs demonstrated an initial upregulation of osteopontin which returned to the baseline level after 6 days. In contrast, osteocalcin showed a sustained upregulation beyond day 3 (Fig. 2D). Transcripts for collagen type I and osteonectin associated with the formation of the extracellular matrix materials were constitutively expressed until day 6 in both basal and osteogenic media and gradually became downregulated (Fig. 2C,D). Both transcripts remained at basal levels during day 9 of osteoblastic differentiation.

In basal conditions, coculturing of BMSCs with PEs actually suppressed the expression of osteopontin and osteocalcin at days 3 and 6, and only enhanced them at day 9, when compared to BMSCs only in basal conditions (Fig. 2A,C). In osteogenic conditions, coculturing of BMSCs with PEs in fact enhanced the expression of these two osteoblasts specific markers (Fig. 2B,D).

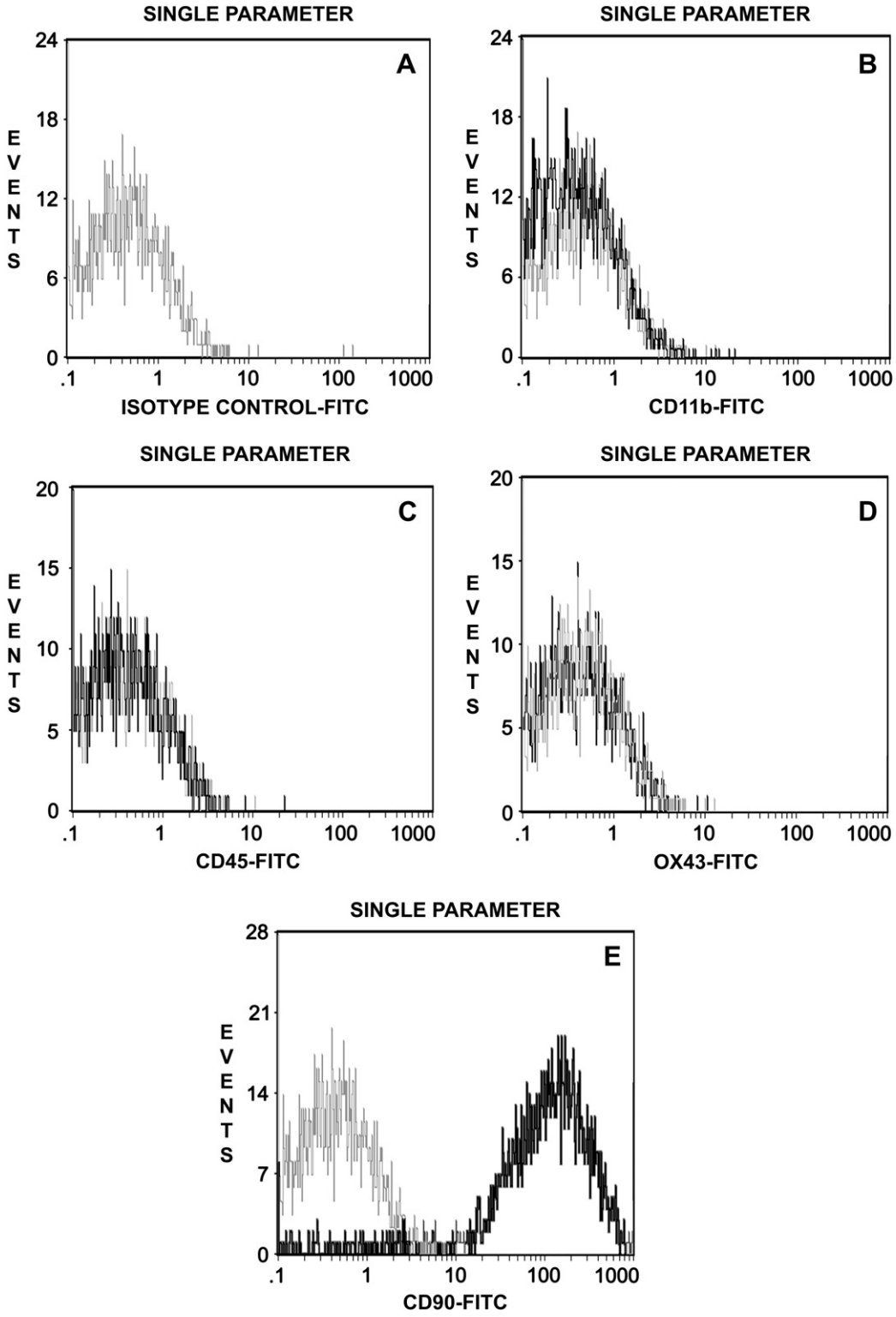

Fig. 1. Immunophenotyping of undifferentiated rat BMSCs by flow cytometry. Passage 3 BMSCs were stained with FITC-conjugated mouse anti-rat CD11b, CD45, CD90, OX43 monoclonal antibodies (black peaks) and, an isotype control, mouse anti-rat FITC-IgG antibody (grey peaks). Isotype control was included in each experiment to identify the level of background fluorescence. Single parameter histograms showing the relative fluorescence intensity of staining on *x*-axis and the number of cells analyzed (events) on the *y*-axis. Isotype control (Panel A). The intensity and distribution of cells stained for hematopoietic and endothelial markers; CD11b (Panel B), CD45 (Panel C) and OX43 (Panel D) were not significantly different from those of isotype control. The fluorescence intensity was greater (shifted to right) when BMSCs were stained with CD90 antibody (black) compared to isotype control (grey). The predominant population of BMSCs homogeneously expressed CD90 surface marker, consistent with their undifferentiated state.

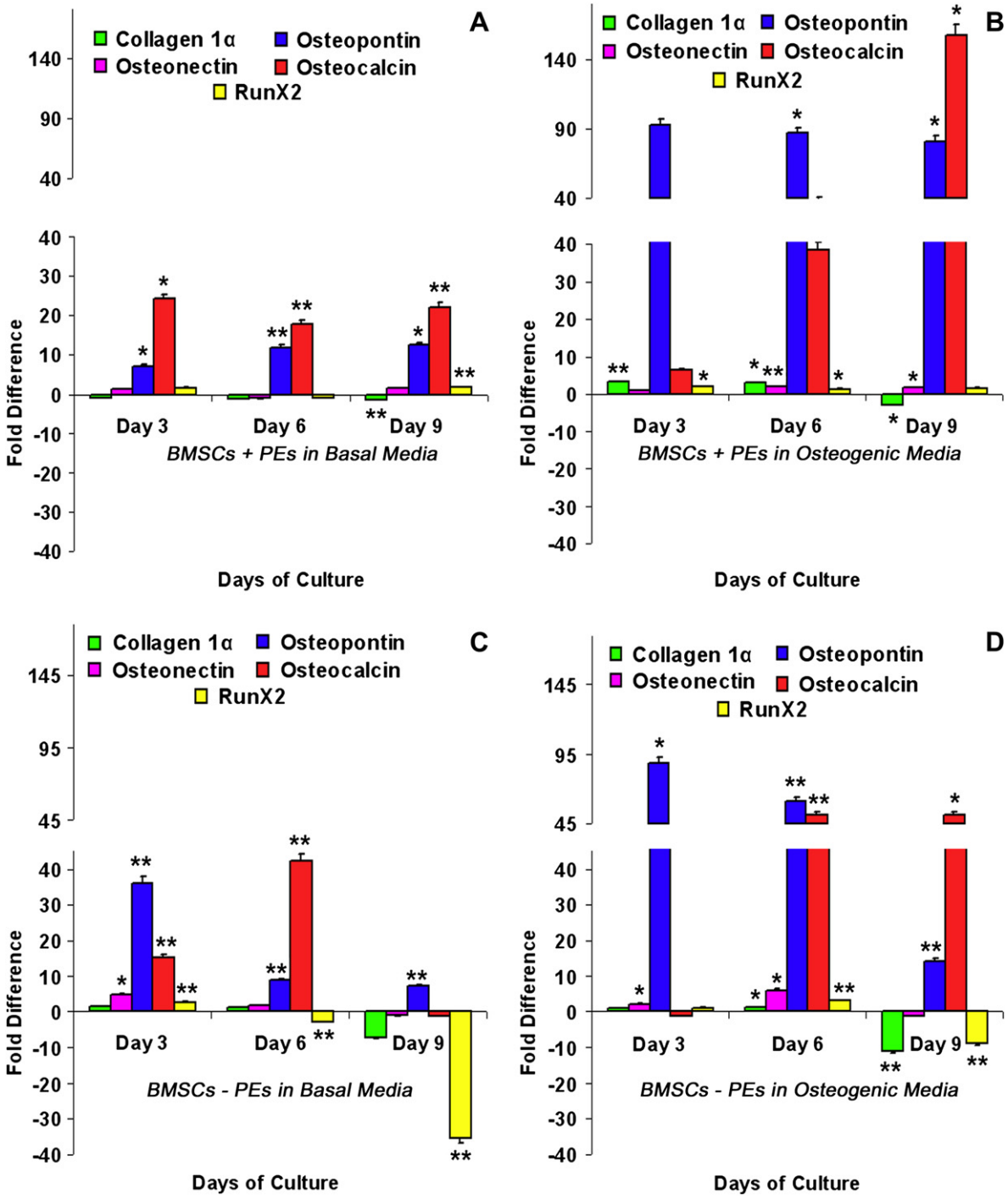

Fig. 2. Real-time reverse transcriptase quantitative polymerase chain reaction (RT-qPCR) analysis of various key osteogenic markers, collagen 1α (Col1a1), osteonectin (Sparc), osteopontin (Spp1), osteocalcin (Bglap2) and runx2 (Runx2) as a function of time. BMSCs and BMSCs/PEs were cultured and maintained as described in the Section 2 and harvested at the time points indicated in the *x*-axis. BMSCs and PEs co-cultured on tubular scaffold in basal media (A) and in osteogenic media (B). BMSCs cultured on the tubular scaffold in basal media (C) and in osteogenic media (D). The C_T (threshold cycle) values were calculated as the average of three replicate measurements for each sample analyzed. The expression ratio was calculated using the REST-XL version 2 software. The values are mean ± SE for three cultures ($n = 3$), $*p < 0.05$; $**p < 0.001$.

3.3. Expression of osteogenic markers in the tubular scaffold

Having demonstrated the expression of osteogenic gene transcripts, their translation products were further investigated in osteogenic tube co-cultures by immunocytochemistry using confocal scanning laser microscopy. The effect of osteogenic media on the accumulation and localization of bone maturation markers was investigated. This was accomplished by staining co-cultures using antibodies directed against alkaline

phosphatase, osteopontin, osteocalcin and osteonectin. BMSCs derived osteoblasts in osteogenic media expressed both early and late stage osteogenic markers. Representative staining patterns obtained for these bone-related proteins are shown in Fig. 3(A–H). Day 9 osteogenic tube co-cultures displayed a distinct phenotype (cuboidal to pear-shaped mononuclear cells) and biosynthetic activity of mature osteoblasts. Predominantly, sheets of osteoblast-like cells were alkaline phosphatase positive and formed multiple foci of concentrically organized cell clusters (Fig. 3A–F). Day 3 and day 6 tube co-cultures demonstrated similar staining for these markers (data not shown). In contrast, cells in non-osteogenic tube co-cultures appeared as interlacing fascicles of elongated cells with little evidence of cellular aggregation amidst the developing vessel-like structures (Fig. 4A–H).

3.4. Characterization of mineralization and nodule formation

One of the hallmarks of osteogenic differentiation is the formation of extracellular mineralized deposits. Confocal microscopic analysis of alizarin red stained day 9 osteogenic co-culture tube sections showed areas of diffuse and nodular mineralization (Fig. 5A–H). By day 9, well-developed sheets of bone-like structures were found throughout the luminal surface of the tubular scaffolds. Fig. 5(A,B) shows the longitudinal sections of tubular scaffolds to expose mineralized nodules on the surface of the lumen and streaks of mineral deposits on the walls. Mineral deposits were evident as early as day 6 with widespread mineralization being present at day 9 in osteogenic cultures. In contrast, no mineralization was observed when BMSCs/PEs were co-cultured on tubular scaffolds in basal media (data not shown) as well as in cell-free collagen-gel tubular scaffolds incubated in osteogenic media for 9 days (Fig. 1S(A,B) in Supplementary data).

3.5. Expression of vasculogenic markers in tubular scaffold

When BMSCs/PEs were co-cultured in the tubular scaffold in osteogenic media for 9 days vessel-like structures were produced (Fig. 6A–L). Immunostaining and confocal microscopic analysis revealed that these structures contained cells that were positive for the vascular antigens QH1 (quail endothelial cells), α-SMA (smooth muscle actin cells), isolectin (endothelial cells) and QCPN (quail cells) (Fig. 6A–L), indicating the origin of quail specific vasculogenic differentiation. An extensive plexus of arborizing capillaries reminiscent of de novo vasculogenesis (endothelial tube formation) was also observed in osteogenic culture conditions (Fig. 6J–L). These elongated and branching thin capillary-like vessels consist of aligned endothelial cells surrounded by α-SMA positive cells. Similarly, when BMSCs/PEs were co-cultured in the tubular scaffold in non-osteogenic media for 9 days, vessel-like structures were observed and demonstrated similar staining pattern for these markers (data not shown).

3.6. Quantitation of alkaline phosphatase and calcium

Alkaline phosphatase and calcium assays were performed to assess the nature and degree of osteoblastic differentiation and matrix mineralization in osteogenic tube co-cultures. Quantitation assays revealed significant increase in alkaline phosphatase activity in osteogenic tube co-cultures/cultures during the observed period of time as compared to control tube co-cultures in basal media (Fig. 7A). In osteogenic tube co-cultures peak alkaline phosphatase activity occurred at day 12. Deposition of calcium was initially observed at day 3. The accumulation significantly increased over time when compared to the tube co-cultures in basal media (Fig. 7B). The level of alkaline phosphatase activity and the accumulation of calcium were proportionately higher in osteogenic tube co-cultures (BMSCs/PEs) when compared to osteogenic tube cultures (BMSCs only; Fig. 7A,B).

4. Discussion

Here we report a novel co-culture of two different types of plastic stem cells, BMSCs (postnatal) and PEs (embryonic), on a 3-D tubular scaffold engineered from aligned collagen type I strands in osteogenic media to generate vascularized bone tissue. It is well established that postnatal bone marrow contains two types of multipotential stem cells, hematopoietic stem cells (HSCs) and mesenchymal stem cells (MSCs). These stem cells exhibit high degree of plasticity. This uniqueness makes bone marrow derived cells an attractive source for tissue engineering that will be at the forefront for future technological developments [29].

Similarly, PE appears to have the potential to vascularize a variety of tissues that has not been adequately tested in vitro. Epicardial progenitors are an extremely plastic type of embryonic tissue that have been proposed to be a multipotent cell lineage [14]. Several recent studies have demonstrated that progenitors of the epicardium and coronary vascular system are derived from extra cardiac tissue, the proepicardial organ (PEO). PEs (coronary progenitor) are easy to isolate and culture, and grow nicely in different in vitro assays [15].

Fate mapping studies show that the proepicardium contains precursors for the endothelium, smooth muscle and adventitial cells (pericytes and fibroblasts) of the coronary vasculature [16]. Formation of coronary vessels occurs by an epithelial to mesenchymal transformation (EMT) of proepicardial cells at the surface of the heart, followed by vasculogenesis in the subepicardial layer, assembly and remodeling of a primitive coronary plexus, and investment by coronary smooth muscle cells [30].

A major challenge for the transplantation of tissue engineered constructs is insufficient oxygen and nutrient supply. Therefore, strategies aiming at the improvement of neovascularization of engineered tissues are of critical importance. A method to enhance graft vascularization is to establish a primitive vascular plexus within the graft before transplantation by the use of cellular-based concepts [31]. Given the complexity of the bone/marrow organ with respect to its structural

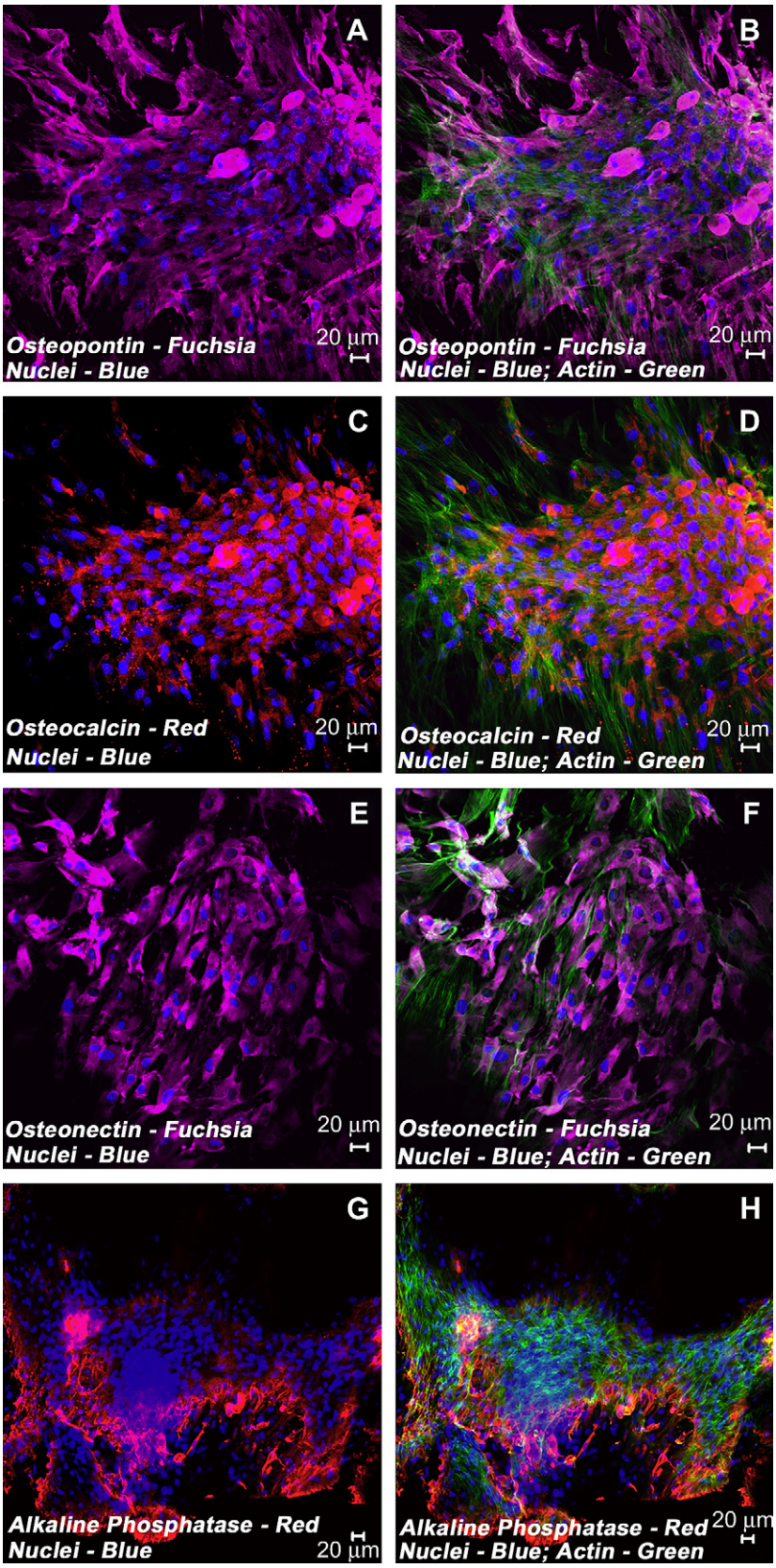

Fig. 3. Expression pattern of various osteogenic markers in tubular scaffold by confocal microscopy. Immunostaining of osteogenic tube co-cultures revealed areas of cellular clustering and aggregation of mature osteoblasts represented by their distinct morphology and phenotypic expression (A–H). Localization of key osteoblastic phenotypic markers of day 9 osteoinductive co-culture tube sections demonstrated the expression of osteopontin (fuchsia, A,B), osteocalcin (red, C,D), osteonectin (fuchsia, E,F), and alkaline phosphatase (red, G,H). Cells were also stained for nuclei (blue, DAPI) and fibrillar actin (green, Alexa 488 phalloidin). Merged images A–H (A–H, scale bar 20 μm).

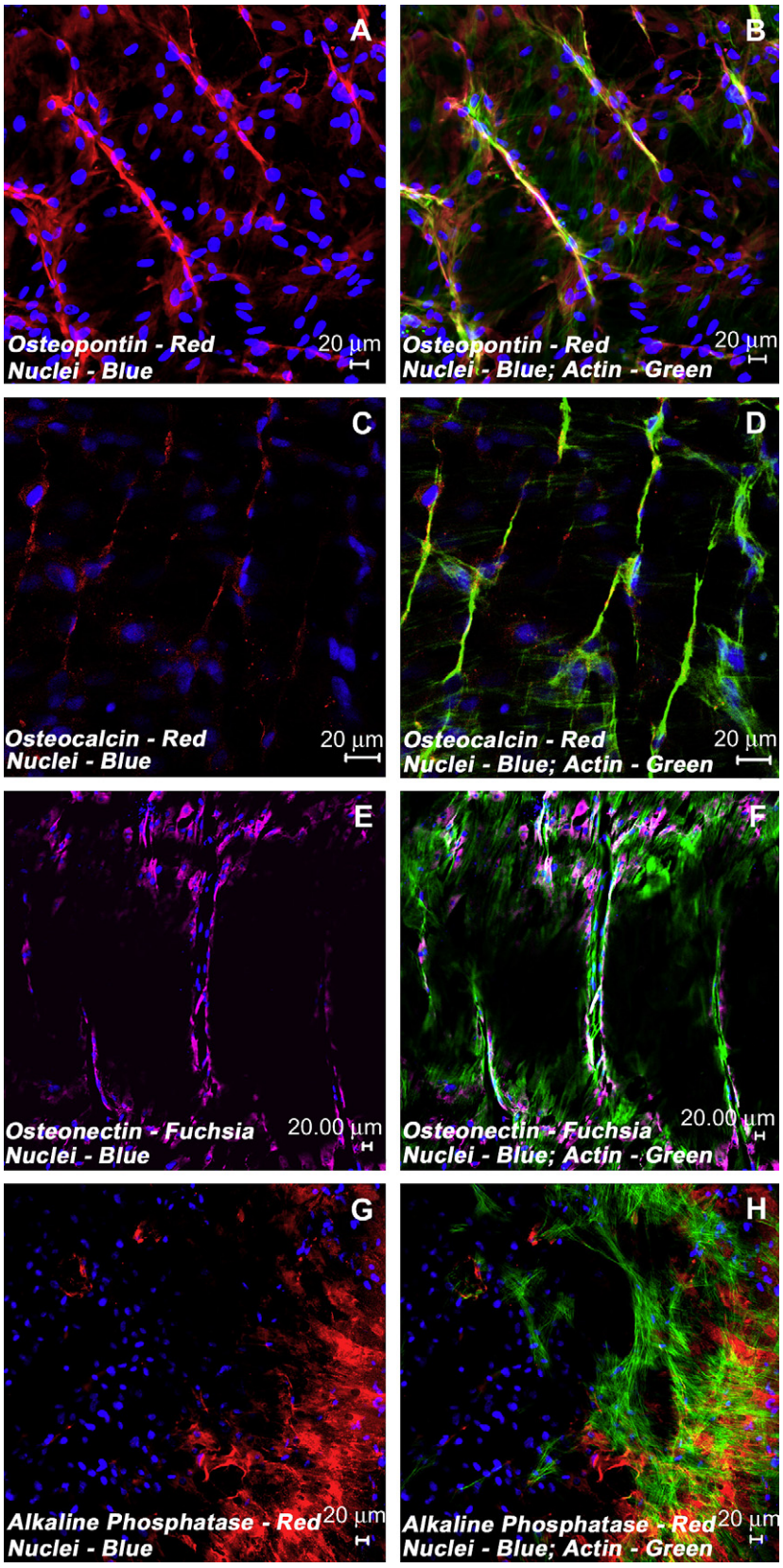

Fig. 4. Expression pattern of various osteogenic markers in tubular scaffold by confocal microscopy. Immunostaining of non-osteogenic tube co-cultures revealed areas of interlacing fascicles of elongated cells with little evidence of cellular aggregation amidst the developing vessel-like structures (A–H, control). Localization of osteoblastic phenotypic markers of day 9 basal tube co-culture sections demonstrated the expression pattern of osteopontin (red, A, B), osteocalcin (red, C, D), osteonectin (fuchsia, E,F), and alkaline phosphatase (red, G,H). Cells were also stained for nuclei (blue, DAPI) and fibrillar actin (green, Alexa 488 phalloidin). Merged images A–H (A–H, scale bar 20 µm).

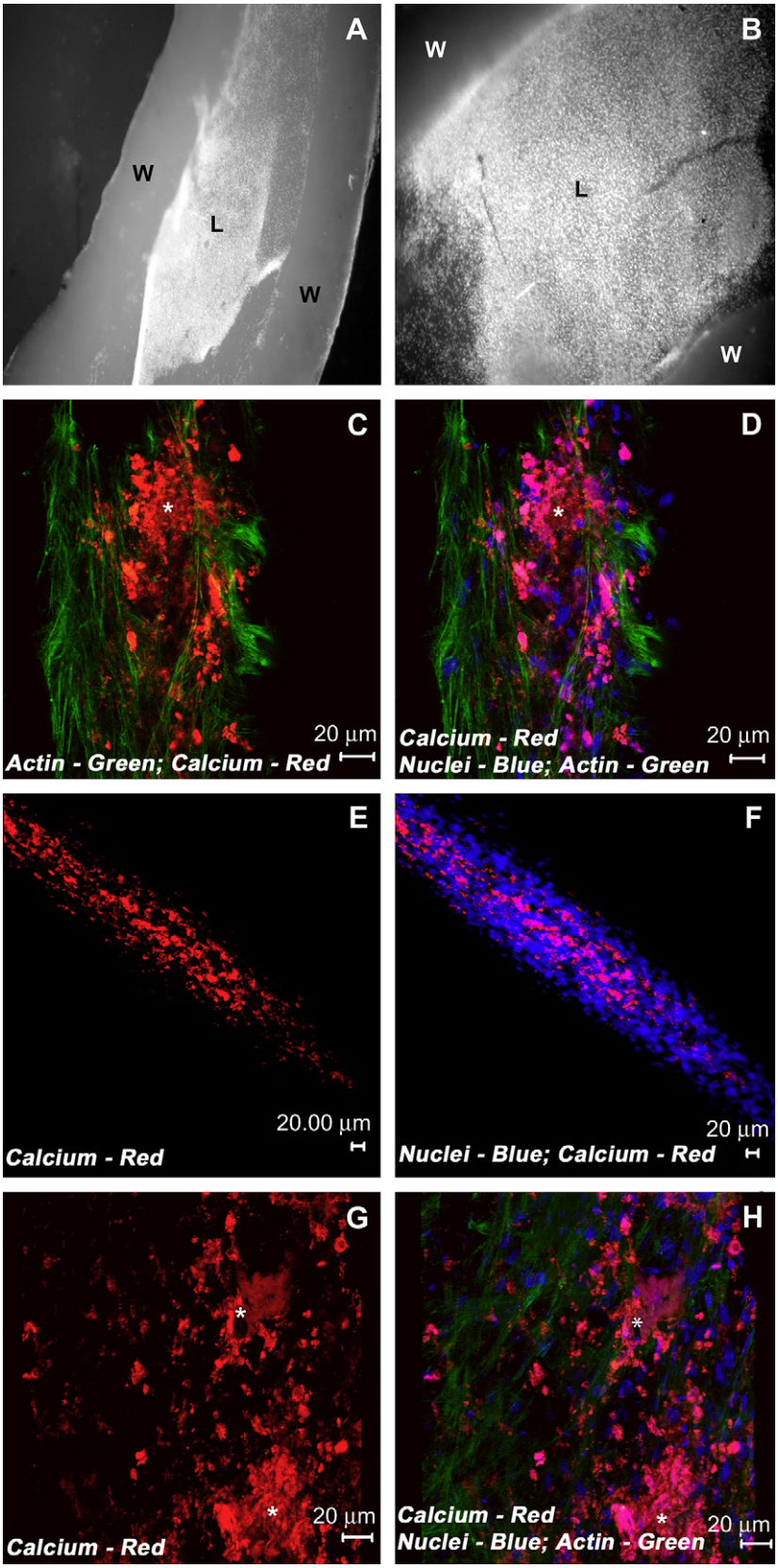

Fig. 5. Pattern of mineralization and nodule formation. Longitudinal sections of the osteogenic co-culture tubes showing areas of extensive mineralization on the luminal surfaces (A,B) (L, lumen; W, wall). Confocal scanning laser microscopic analysis of mineralized matrix by Alizarin red staining for calcium demonstrated extensive areas of diffuse and nodular (C,G, white asterisks) mineralization of the collagen-gel tubular scaffolds. Sections of day 9 osteoinductive co-culture tubes were stained for calcium (red, Alizarin red; C,E,G) revealing the mineralized extracellular matrix materials. Cells were also stained for nuclei (blue, DAPI) and fibrillar actin (green, Alexa 488 phalloidin). Images (E) and (F) were projections representing 64 sections collected at 4.96 µm intervals. Images (G) and (H) were projections representing 20 sections collected at 5 µm intervals. Merged images (C,D,F,H). (C−H, scale bar 20 µm.)

organization and relationships between various different cell types within it, and its reliance on the vasculature, true differentiation cannot be achieved by any in vitro protocol, including those that incorporate the cells within a 3-D structure. However, some initial insight can be delineated from in vitro differentiation assays [32].

Most approaches to engineering new tissue have relied on the host for vascularization. Although this approach has been moderately successful, it has not proven effective in thick highly vascularized tissues such as muscle [33]. One of the major challenges in engineering complex tissues such as bone, which involves the reconstruction of 3-D shapes and internal architectures, is the need to vascularize the tissue in vitro. Vascularization in vitro could maintain cell viability during tissue growth, induce structural organization and promote vascularization upon implantation. Vascular arrangement of the overlying periosteum precedes and dictates the architecture of the new bone. Ripamonti et al. proposed that preconstruction of an appropriate vasculature and scaffold with pore size and surface architecture conducive to the growth of vessels is of paramount significance [7,8,34].

We hypothesized that embryonic PEs in the appropriate environment could be used to induce endothelial vessel networks in engineered bone tissue in vitro. The avian PE was investigated initially because it is readily amenable to dissection [35] and well-developed antibodies are available for characterizing the vascular components. Hence, first we developed a 3-D co-culture system in which rat BMSCs were co-seeded with quail PEs and cultured on a highly aligned, porous, biocompatible collagen-gel tubular scaffold for differentiation purposes. Here, we compared the effects of two types of growth media, osteogenic and basal media, in addition we compared and specifically assessed the consequence of PEs presence on the expression of osteogenic markers in BMSCs. Osteogenic media promoted the osteoblastic differentiation of the BMSCs and also supported the formation of endothelium lined tube-like structures within the constructs, whereas basal medium alone generated vessel-like structures within the constructs and did not support the differentiation of BMSCs into osteoblasts.

Three principle periods of the osteoblast developmental sequence are defined: proliferation, matrix development and maturation, and mineralization. Several genes associated with formation of the ECM such as collagen type I, fibronectin, and transforming growth factor β (TGF-β) are actively expressed during the proliferative phase of developing osteoblasts and then gradually downregulated. Collagen type I mRNA is maintained at basal level during subsequent stages of osteoblastic differentiation. As proliferation decreases, genes associated with matrix development and maturation are upregulated. The formation of this mature ECM in turn, downregulates proliferation, and allows for mineralization process to begin. This mineralization in turn downregulates the expression of genes associated with the ECM maturation [36].

Proliferation of osteoblasts in a cell culture system depends on the density of the seeded cells and their inherent division potential as well as the type of substrates on which they are cultured. It has been shown that when primary diploid fetal calvarial-derived osteoblasts were cultured on collagen type I film or in collagen-gel substrates, the cells receive cues and/or inductive signals from the ECM which leads to an accelerated progression of osteoblastic phenotype. This is seen in a decline in proliferative activity and the subsequent induction of genes associated with matrix maturation and mineralization of the developing osteoblasts [37].

To study the expression pattern of key osteogenic gene transcripts in the 3-D tube constructs, we analyzed the expression of collagen type I, osteonectin, osteopontin, osteocalcin and Runx2 at mRNA level in the tube constructs. RT-qPCR results showed that osteoblastic differentiation of BMSCs in osteogenic conditions resulted in increased expression of non-collagenous proteins such as osteopontin (bone sialoprotein) and osteocalcin specific of osteoblasts. Moreover, co-cultures that included BMSCs/PEs had higher levels of osteopontin and osteocalcin mRNAs than BMSCs alone. The increased expression of the osteoblast-specific structural gene, osteocalcin, which is only expressed by fully differentiated osteoblasts by day 9, is consistent with the observed endothelial networks in the co-culture. This could possibly be one of the necessary factors regulating the induction of mature osteoblasts/mineralization of the constructs and may not be sufficient on its own.

As indicated by immunostaining for various osteogenic markers, day 9 tube cultures showed that BMSCs were able to adhere, proliferate and migrate and undergo complete maturation and differentiation into osteoblasts and formed highly cohesive cellular aggregates. These cellular aggregates were alkaline phosphatase and osteocalcin positive. Furthermore, these cellular aggregations culminated into mineralized bone-like nodules. When BMSCs and PEs were co-cultured on the scaffolds, the PEs organized into tube-like structures amidst developing osteoblasts throughout the construct, forming vessel-like networks within the engineered bone tissue in vitro.

It has been suggested that mineral formation that occurs in the presence of supersaturated β-glycerophosphate conditions may be non-physiological, if it exceeds 2 mM. Chung and co-workers [38] using a cell-free system demonstrated that mineral particles formed spontaneously in the presence of alkaline phosphatase and β-glycerophosphate and were deposited into a collagen matrix. However, this phenomenon was not observed in our cell-free collagen-gel tubular scaffolds when incubated in osteogenic media supplemented with 10 mM β-glycerophosphate for 9 days. This suggests that the mineralization observed in osteogenic culture conditions is predominantly due to a cell-mediated event and not the result of random precipitation.

PEs derived vessel formation is a combination of vasculogenesis, de novo endothelial tube formation, and angiogenesis, sprouting from existing endothelial tubes [39]. Blood vessels are stabilized by association with pericytes or smooth muscle cells [40,41]. In this study, we have demonstrated that the isolated PEs were able to adhere and proliferate in the tubular scaffold in osteogenic conditions and continue their

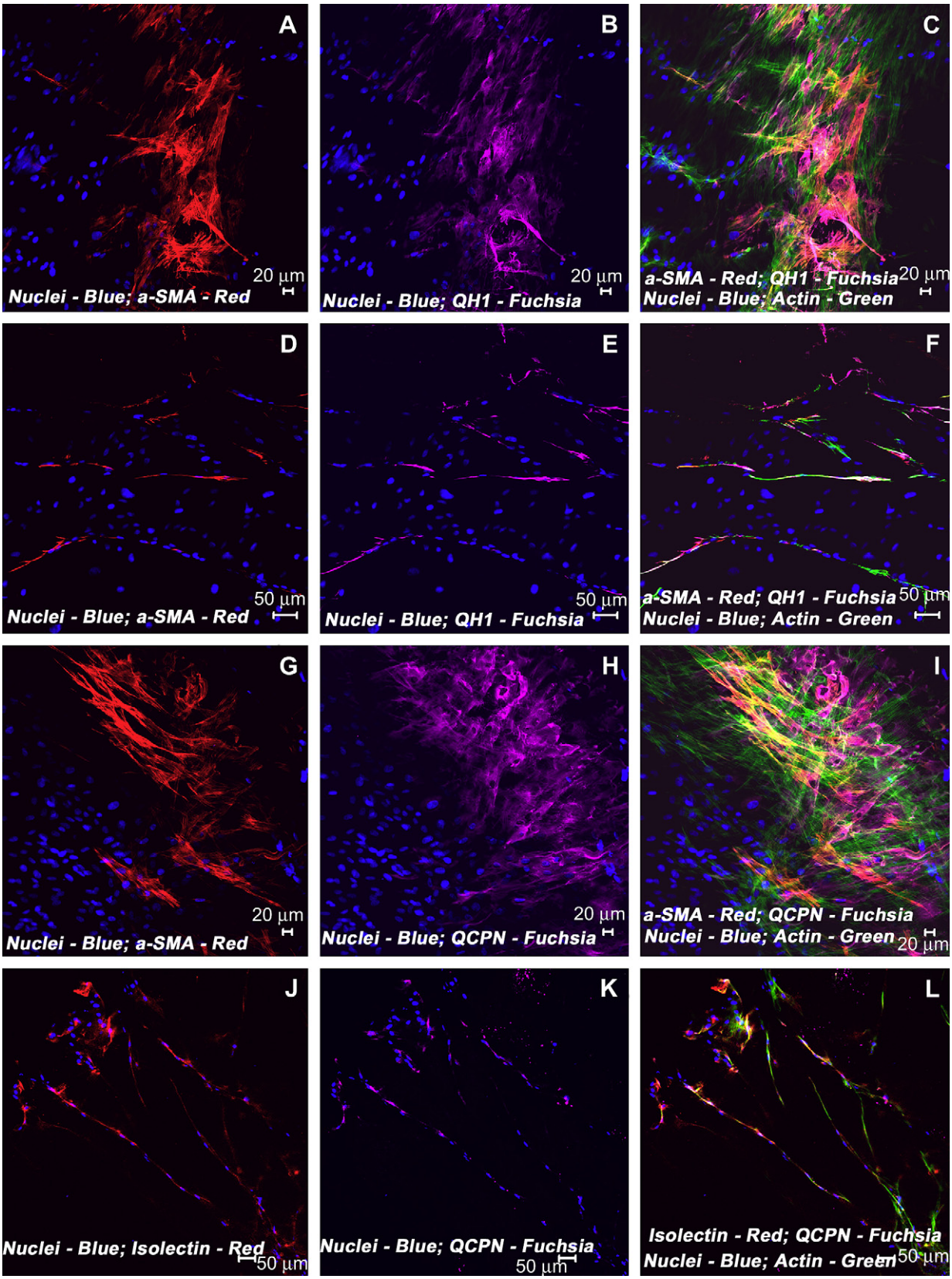
A
Nuclei - Blue; a-SMA - Red
20 μm
B
Nuclei - Blue; QH1 - Fuchsia
20 μm
C
a-SMA - Red; QH1 - Fuchsia
Nuclei - Blue; Actin - Green
20 μm
D
Nuclei - Blue; a-SMA - Red
50 μm
E
Nuclei - Blue; QH1 - Fuchsia
50 μm
F
a-SMA - Red; QH1 - Fuchsia
Nuclei - Blue; Actin - Green
50 μm
G
Nuclei - Blue; a-SMA - Red
20 μm
H
Nuclei - Blue; QCPN - Fuchsia
20 μm
I
a-SMA - Red; QCPN - Fuchsia
Nuclei - Blue; Actin - Green
20 μm
J
Nuclei - Blue; Isolectin - Red
50 μm
K
Nuclei - Blue; QCPN - Fuchsia
50 μm
L
Isolectin - Red; QCPN - Fuchsia
Nuclei - Blue; Actin - Green
50 μm

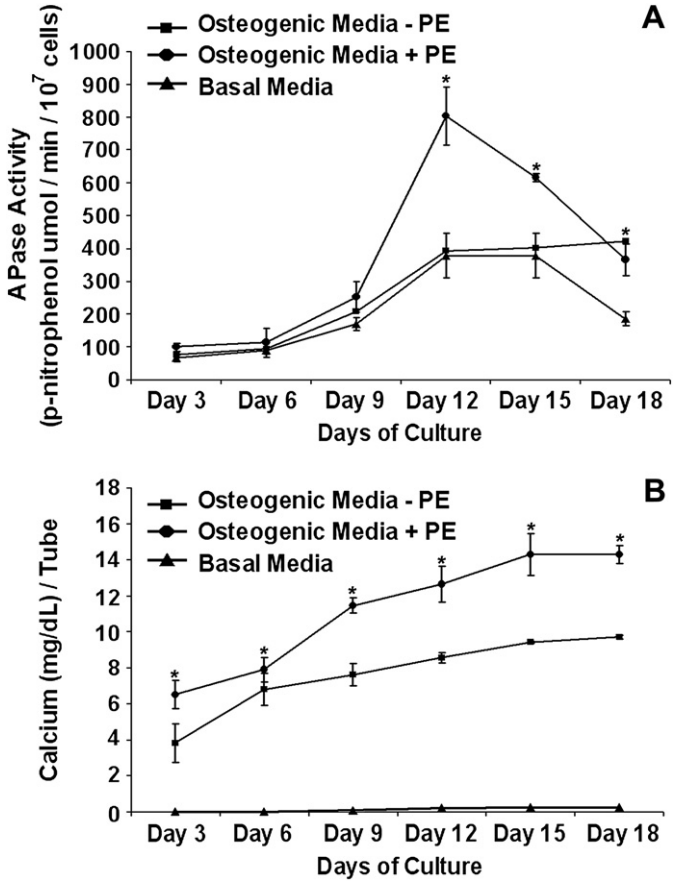

Fig. 7. Osteogenic differentiation of BMSCs/PEs co-culture in 3-D collagen-gel tubular scaffolds. Osteogenic differentiation of BMSCs over a period of 18 days was demonstrated by the increase in alkaline phosphatase and the deposition of minerals. (A) The quantification of alkaline phosphatase demonstrated an increase in activity over 18 days. $*p < 0.05$. The data represent the mean ± SEM of duplicate cultures ($n = 2$). (B) The quantification of calcium indicated that the accumulation continued beyond 14 days. $*p < 0.05$. The data represent the mean ± SEM of duplicate cultures ($n = 2$).

development to undergo vessel-like formation. To identify definitive endothelial cells, the QH1 antibody, which identifies quail endothelial cells, was used [42]. In addition, isolectin, another marker for endothelial cells, was found closely associated with QH1 staining. These two endothelial-specific markers localized to capillary-like structures present on and within the scaffold. This suggests that PE-derived endothelial cells coalesced into endothelial tube-like structures and began the process of vasculogenesis, consistent with our previous study [19]. The PE-derived cells and the vessel-like structures expressed α-SMA, and these α-SMA positive cells were recruited in juxtaposition to the aligned endothelial cells and they wrapped around in an orientation that resembles in vivo vessel-like structures. Further work is in progress to elucidate the vessel maturation, like a patent lumen formation, and their functional capabilities and utilization of mammalian derived PEs, especially from rat. Finally, our molecular, biochemical, immunocytochemical and histomorphological data show that the specific geometric configuration of the 3-D collagen-gel tubular scaffold in the form of aligned fibers is the driving microenvironment conducive and inductive to the sequence of differentiation events culminating into vascularized, mineralized bone-like elements.

5. Conclusions

Here we report the development of a novel co-culture that recapitulates many aspect of osteogenesis. Since BMSCs/PEs synergetically differentiated into both osteoblastic and vascular cell lineages, this in vitro model system provides a platform for investigating the functional role and interplay of neovascularization in the maturation and differentiation of BMSCs derived osteoblasts as well as to study the factors that regulate angiogenesis, vasculogenesis and vessel maturation. Besides, in vitro engineering of vascularized bone as replacement tissue for small segmental bone defects in regenerative medicine.

6. Disclosures

All authors have no conflicts of interest.

Acknowledgments

The authors thank Dr. Robert L. Price for his critical reading of the manuscript, Dr. Gene Mayer for flow cytometric analysis, and Mr. David Farr and Ms. Cheryl Cook for their excellent technical assistance. The monoclonal antibodies were obtained for this study from the Developmental Studies Hybridoma Bank (DSHB) developed under the auspices of the NICHD and maintained by The University of Iowa, Department of Biological Sciences, Iowa City, IA 52242; and National Heart, Lung, and Blood Institute (NHLBI) is highly acknowledged.

Fig. 6. Expression pattern of various vasculogenic markers in tubular scaffold by confocal microscopy. Immunostaining revealed areas of abundant interlacing fascicles of QCPN, QH1, isolectin and α-smooth muscle actin (α-SMA) positive cells in osteogenic tube co-cultures (A–L). In addition, extensive arborizations of nascent capillary-like structures were also seen amidst the developing cellular aggregates. Localization of key vasculogenic phenotypic markers of day 9 osteoinductive co-culture tube sections demonstrated the expression of α-SMA (red, A,D,G), QH1 (fuchsia, B,E), QCPN (fuchsia, H,K) and isolectin (red, J). The merged images showing the actin cytoskeleton (green) are shown in panels C, F, I and L. Sections of a day 9 osteogenic tube culture demonstrated nascent capillary-like structures positive for α-SMA (red, D) and QH1 (fuchsia, E). These elongated cord-like structures showed colocalization of α-SMA, QH1 and actin (merged, F). In the tubes nuclei appeared aligned (blue, DAPI). Similar sections of osteogenic co-cultured tubes illustrate the sprouting and branching tube-like structures positive for the endothelial marker isolectin (red, J) and QCPN (fuchsia, K). This plexus contained arborizing capillary-like vessels lined with quai endothelial cells and showed colocalization of isolectin, QCPN and actin (merged, L). Cells were also stained for nuclei (blue, DAPI) and fibrillar actin (green, Alexa 488 phalloidin). Merged images A–L (A–C, G–I, scale bar 20 μm; D–F, J–L, scale bar 50 μm).

Appendix. Supplementary data

Supplementary data associated with this article can be found in the online version, at doi:10.1016/j.biomaterials.2007.07.004.

References

[1] Friedenstein AJ, Piatetzky-Shapiro II, Petrakova KV. Osteogenesis in transplants of bone marrow cells. J Embryol Exp Morphol 1966;16:381–90.

[2] Friedenstein AJ, Petrakova KV, Kurolesova AI, Frolova GP. Heterotopic transplants of bone marrow: analysis of precursor cells for osteogenic and hematopoietic tissues. Transplantation 1968;6:230–47.

[3] Friedenstein AJ, Gorskaja JF, Kulagina NN. Fibroblast precursors in normal and irradiated mouse hematopoietic organs. Exp Hematol 1976;4:267–74.

[4] Beresford JN, Bennett JH, Devlin C, Leboy PS, Owen ME. Evidence for an inverse relationship between the differentiation of adipocytic and osteogenic cells in rat marrow stromal cell cultures. J Cell Sci 1992;102:341–51.

[5] Pereira RF, Halford KW, O'Hara MD, Leeper DB, Sokolov BP, Pollard MD, et al. Cultured adherent cells from marrow can serve as long-lasting precursor cells for bone, cartilage, and lung in irradiated mice. Proc Natl Acad Sci USA 1995;92:4857–61.

[6] Maniatopoulos C, Sodek J, Melcher AH. Bone formation in vitro by stromal cells obtained from bone marrow of young adult rats. Cell Tissue Res 1988;254:317–30.

[7] Ripamonti U, Ramoshebi LN, Patton J, Matsaba T, Teare J, Renton L. Soluble signals and insoluble substrata: novel molecular cues instructing the induction of bone. In: Massaro EJ, Rogers JM, editors. The skeleton. Totowa, NJ: Humana Press; 2004. p. 217–27.

[8] Ripamonti U. Soluble, insoluble and geometric signals sculpt the architecture of mineralized tissues. J Cell Mol Med 2004;8:169–80.

[9] Reddi AH. Role of morphogenetic proteins in skeletal tissue engineering and regeneration. Nat Biotechnol 1998;16:247–52.

[10] Carano RA, Filvaroff EH. Angiogenesis and bone repair. Drug Discov Today 2003;8:980–9.

[11] Lanza RP, Langer R, Vacanti J. Principles of tissue engineering. San Diego, CA: Academic Press; 2000.

[12] Villanueva JE, Nimni ME. Promotion of calvarial cell osteogenesis by endothelial cells. J Bone Miner Res 1990;5:733–9.

[13] Carvalho RS, Einhorn TA, Lehmann W, Edgar C, Al-Yamani A, Apazidis A, et al. The role of angiogenesis in a murine tibial model of distraction osteogenesis. J Artif Organs 2004;34:849–61.

[14] Perez-Pomares JM, Mironov V, Guadix JA, Macias D, Markwald RR, Munoz-Chapuli R. In vitro self-assembly of proepicardial cell aggregates: an embryonic vasculogenic model for vascular tissue engineering. Anat Rec A Discov Mol Cell Evol Biol 2006;288:700–13.

[15] Wessels A, Perez-Pomares JM. The epicardium and epicardially derived cells (EPDCs) as cardiac stem cells. Anat Rec A Discov Mol Cell Evol Biol 2004;276:43–57.

[16] Tomanek RJ. Formation of the coronary vasculature during development. Angiogenesis 2005;8:273–84.

[17] Perez-Pomares JM, Carmona R, Gonzalez-Iriarte M, Atencia G, Wessels A, Munoz-Chapuli R. Origin of coronary endothelial cells from epicardial mesothelium in avian embryos. Int J Dev Biol 2002;46:1005–13.

[18] Guadix JA, Carmona R, Munoz-Chapuli R, Perez-Pomares JM. In vivo and in vitro analysis of the vasculogenic potential of avian proepicardial and epicardial cells. Dev Dyn 2006;235:1014–26.

[19] Nesbitt TL, Patel PA, Yost MJ, Goodwin RL, Potts JD. A 3-D model of coronary vessel development. In Vitro Cell Dev Biol Anim 2007;43:10–6.

[20] Yost MJ, Baicu CF, Stonerock CE, Goodwin RL, Price RL, Davis JM, et al. A novel tubular scaffold for cardiovascular tissue engineering. Tissue Eng 2004;10:273–84.

[21] Hamburger V, Hamilton HL. A series of normal stages in the development of the chick embryo. J Morphol 1951;88:49–92.

[22] Bustin SA. Absolute quantification of mRNA using real-time reverse transcription polymerase chain reaction assays. J Mol Endocrinol 2000;25:169–93.

[23] Pfaffl MW. A new mathematical model for relative quantification in real-time RT-PCR. Nucleic Acids Res 2001;29:e45.

[24] Pfaffl MW, Horgan GW, Dempfle L. Relative expression software tool (REST) for group-wise comparison and statistical analysis of relative expression results in real-time PCR. Nucleic Acids Res 2002;30:e36.

[25] Pfaffl MW, Tichopad A, Prgomet C, Neuvians TP. Determination of stable housekeeping genes, differentially regulated target genes and sample integrity: BestKeeper – Excel-based tool using pair-wise correlations. Biotechnol Lett 2004;26:509–15.

[26] Potts JD, Dagle JM, Walder JA, Weeks DL, Runyan RB. Epithelial-mesenchymal transformation of embryonic cardiac endothelial cells is inhibited by a modified antisense oligodeoxynucleotide to transforming growth factor beta 3. Proc Natl Acad Sci USA 1991;88:1516–20.

[27] Kihara T, Hirose M, Oshima A, Ohgushi H. Exogenous type I collagen facilitates osteogenic differentiation and acts as a substrate for mineralization of rat marrow mesenchymal stem cells in vitro. Biochem Biophys Res Commun 2006;341:1029–35.

[28] Pittenger MF, Mackay AM, Beck SC, Jaiswal RK, Douglas R, Mosca JD, et al. Multilineage potential of adult human mesenchymal stem cells. Science 1999;284:143–7.

[29] Bianco P, Robey PG. Stem cells in tissue engineering. Nature 2001;414:118–21.

[30] Majesky MW. Development of coronary vessels. Curr Top Dev Biol 2004;62:225–59.

[31] Finkenzeller G, Torio-Padron N, Momeni A, Mehlhorn AT, Bjorn Stark G. In vitro angiogenesis properties of endothelial progenitor cells: a promising tool for vascularization of ex vivo engineered tissues. Tissue Eng 2007;13:1413–20.

[32] Bianco P, Kuznetsov SA, Riminucci M, Robey PG. Postnatal skeletal stem cells. Methods Enzymol 2006;419:117–48.

[33] Levenber S, Rouwkema J, Macdonald M, Garfein ES, Kohane DS, Darland DC, et al. Engineering vascularized skeletal muscle tissue. Nat Biotechnol 2005;23:879–84.

[34] Yoshikawa H, Myoui A. Bone tissue engineering with porous hydroxyapatite ceramics. J Artif Organs 2005;8:131–6.

[35] Antin P, Fallon JF, Schoenwolf GC. The chick embryo rules (still)! Dev Dyn 2004;229:413.

[36] Lian JB, Stein GS, Owen TA, Tassinari MS, Aronow M, Collart D, et al. Gene expression during development of the osteoblast phenotype: an integrated relationship of cell growth to differentiation. In: Stein GS, Lian JB, editors. Molecular and cellular approaches to the control of proliferation and differentiation. San Diego: Academic Press; 1992. p. 165–223.

[37] Stein GS, Lian JB, Owen TA, Holthuis J, Bortell R, van Wijnen AJ. Molecular mechanisms that mediate a functional relationship between proliferation and differentiation. In: Stein GS, Lian JB, editors. Molecular and cellular approaches to the control of proliferation and differentiation. San Diego: Academic Press; 1992. p. 299–341.

[38] Chung CH, Golub EE, Forbes E, Tokuoka T, Shapiro IM. Mechanism of action of beta-glycerophosphate on bone cell mineralization. Calcif Tissue Int 1992;51:305–11.

[39] Wada AM, Smith TK, Osler ME, Reese DE, Bader DM. Epicardial/mesothelial cell line retains vasculogenic potential of embryonic epicardium. Circ Res 2003;92:525–31.

[40] Koike N, Fukumura D, Gralla O, Au P, Schechner JS, Jain RK. Tissue engineering: creation of long-lasting blood vessels. Nature 2004;428:138–9.

[41] Carmeliet P. Angiogenesis in health and disease. Nat Med 2003;9:653–60.

[42] Pardanaud L, Altman C, Kitos P, Dieterlen-Lievre F, Buck CA. Vasculogenesis in the early quail blastodisc as studied with a monoclonal antibody recognizing endothelial cells. Development 1987;100:339–49.